LAMINAR FLOW IN THE ENTRANCE REGION OF AN ANNULAR CHANNEL WITH DISSIPATION

T. Gopal Reddy*

M. Rama Chandra Reddy**

B. Rama Bhupal Reddy***

Abstract:

In this paper we analyze the Laminar flow in the entrance region of an annular channel with dissipation. The motion of fluid is between the two insulating cylinders which are concentric. The origin of the coordinate system is located at the extreme left of the channel along the central line of the cylinders, Z is the coordinate which increases in the down stream direction, R is the radial coordinate and θ is the angular coordinate and is perpendicular to the (R, Z) plane. The flow problem is described by means of partial differential equations and the solutions are obtained by using an implicit finite difference technique. The velocity, temperature and pressure profiles are obtained and their behaviour is discussed computationally for different values of governing parameters like Eckert number Ek and Prandtl number Pr.

Keywords: Laminar flow, Dissipation, Annual Channel

* Jr. Lecturer in Mathematics, Government Junior College, Kurnool, A.P., India.

** Reader in Mathematics, S.K.S.C. Degree College, Proddatur, A.P., India.

*** Associate Professor in Mathematics, K.S.R.M. College of Engineering, Kadapa, A.P., India.

1. INTRODUCTION

Internally finned tubes are commonly used as efficient means of augmenting convective heat transfer in tubular heat exchangers. A number of numerical investigations have been performed for the heat transfer and pressure drop characteristics in fully developed regions of various internally finned tubes [2, 10, 17, 21, 22, 24, 26, 27]. For laminar developing flow and heat transfer in a circular tube with internal longitudinal fins, numerical simulations have been conducted [11, 18, 19] assuming the flow to be parabolic in the axial direction. In circular and annular tubes with longitudinal fins there are two limiting cases which are widely used in engineering. One is the sector duct, which can be considered as the limiting case of a circular tube with its longitudinal continuous fins spanning the full length of the radius. The other is the annular-sector duct [3], for which the fins in annulus span the full width of the annulus. The numerical analysis of the developing fluid flow and heat transfer in the circular-sector duct was conducted by Lei and Trupp [10] and Chung and Hsia [5]. Although the fully developed fluid flow and heat transfer in the annular-sector duct has been performed by several authors [2, 6, 15, 23], no results are provided in the literature for the developing region.

The thermally developing laminar flow and heat transfer in ducts of different cross sections continue to be an interesting subject in recent literature [7, 11, 29], but the developing situation in the annular-sector duct is still not involved. The annular-sector duct may be considered as one sub-channel of a multipassage annular tube, which is used in the intercooler of gas compressors for the cooling of pressurized gas, in double-pipe heat exchangers, etc. The aim of the present study is to predict numerically the developing laminar flow and heat transfer through annular-sector ducts with apex angles ranging from 18^o to 40^o. Using the control-volume-based, fully implicit, finite difference method, the procedure used in the present study is basically the same as proposed by Patankar and Spalding [16], except that the discretization scheme for the convection-diffusion terms in the cross section is the power-law scheme. Sparrow et.al. [25] studied the analytical solution for the annular sector duct. Chiranjivi and Vidyanidhi [4] studied analytical solution for the annular sector duct. Conventionally [20], the hydrodynamic entrance length L is defined as the distance for the axial velocity at the center line to reach 99%of the fully developed value. This length may also be defined in terms of the distance required for $K(z)$ to approach its fully developed value within a pre-assigned percentage (i.e., 99%) [1]. As claimed

in many heat transfer text books, such as [8], if Pr< 1 the thermal boundary layer in internal flow develops more rapidly than the hydrodynamic boundary layer.

Several researchers investigated the problem of laminar flow forced convection in ducts of various cross-sections during 1950 through 1970. Solutions for developing and developed velocity and temperature profiles, by various exact analytical and approximate methods are available in the literature. Experimental results are also available for different flow geometries. An extensive review of these solutions is presented by Shah and London [20]. Several investigators are continuing studies on laminar flow convective heat transfer in non-circular ducts. Uzun and Unsal[28] presented a numerical solution for laminar heat conduction in ducts of irregular cross-sections. The solutions of heat transfer to a power law fluid in arbitrary cross-sectional ducts was presented by Uzun[30]. Muzychka and Yovanovich [13, 14] reviewed the laminar flow friction and heat transfer in non-circular ducts and the same authors [12] proposed a new model for predicting Nusselt numbers for laminar forced convection heat transfer in the combined entry region of non-circular ducts. The performance of the numerical work in predicting the velocity field of some industrial problems has become increasingly important. The flow in ducts occurs in many industrial applications, such as compact heat exchangers, nuclear reactors and gas turbine cooling systems. However, the flow in these cooling passages is considered turbulent. Many fundamental studies of the flow in straight ducts can be found. The researchers in these studies emphasis on the velocity and temperature fields, hydraulic parameters such as Nusselt number, Reynolds number.

In this paper determines the velocity and temperature of laminar flow in the entrance region of an annular channel. Both the velocity and temperature profiles are initially flat upon entering channel. The equations of the system are place into a finite difference form and solved numerically for various Eckert number Ek and fixed Prandtl number Pr. Velocity, temperature and pressure curves are presented from the results of computational work.

2. NOMENCLATURE

C_P	Specific heat
E_k	Eckert Number
P	Dimensionless pressure difference
Pr	Prandtl number

r	Axial Co-ordinate
R	Dimensionless axial Co-ordinate
T	Temperature
T_{in}	Input temperature
T_W	Wall temperature
u_0	Uniform input velocity
u_r	Axial Velocity Component
u_z	Transverse Velocity Component
U	Dimensionless stream-wise velocity
V	Dimensionless transverse velocity
z	Transverse Co-ordinate
Z	Dimensionless Transverse Co-ordinate
ρ	Mass density
κ	Thermal Conductivity
μ	Dynamic viscosity
θ	Dimensionless Temperature

3. FORMULATION OF THE PROBLEM

The annular device is shown in figure 1. This representation is best described in cylindrical coordinates. The motion of the fluid is between the two insulating cylinders, which are concentric. The origin of the co-ordinate system is located at the extreme left of the channel along the center line of the cylinders, Z is the co-ordinate which increases in the down stream direction, r is the radial co-ordinate and θ is the angular co-ordinate and is perpendicular to the (r, z) plane. Note that the origin of this co-ordinate system is not placed in the center of the region in which the fluid passes. The uniform magnetic field will be in the radial direction. The inner radius of the channel is r_i and the outer radius is r_0. Te channel is of length '*L*', which must be long compared with the entry length.

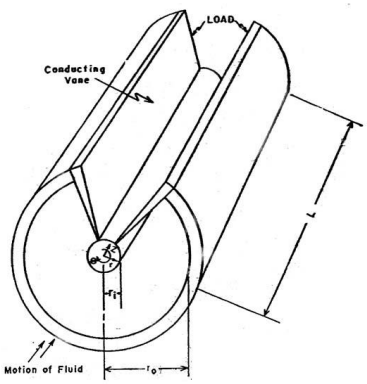

Figure 1 Annual channel configuration

The governing equations are:

$$\frac{D\rho}{Dt} + = \frac{\partial \rho}{\partial \tau} + \bar{q} \cdot \nabla \rho \qquad (1)$$

$$\rho \frac{Dq}{Dt} = -\nabla p + \mu \nabla^2 \bar{q} \qquad (2)$$

$$\rho \, C_p \left[\bar{q} \cdot \nabla \right] T = \kappa \nabla^2 T + \phi \qquad (3)$$

Where ϕ = Dissipation function

$$= \mu \left(\frac{\partial u_r}{\partial z} + \frac{\partial u_z}{\partial r} \right)^2 + 2\mu \left[\left(\frac{\partial u_r}{\partial r} \right)^2 + \left(\frac{\partial u_z}{\partial z} \right)^2 \right]$$

The following assumptions are made:

(i) Flow is steady, laminar, viscous, incompressible and developed.

(ii) All the physical properties of the fluid are assumed to be constant

The resultant equations in cylindrical coordinates from the above assumptions are listed below:

$$\frac{1}{r} \frac{\partial (r.u_r)}{\partial r} + \frac{\partial u_z}{\partial z} = 0 \qquad (4)$$

$$\rho\left[u_r\frac{\partial u_z}{\partial r}+u_z\frac{\partial u_z}{\partial z}\right]=-\frac{\partial p}{\partial z}+\mu\left[\frac{\partial^2 u_z}{\partial r^2}+\frac{1}{r}\frac{\partial u_z}{\partial r}\right] \quad (5)$$

$$\rho C_P\left[u_r\frac{\partial T}{\partial r}+u_z\frac{\partial T}{\partial z}\right]=\kappa\left[\frac{\partial^2 T}{\partial r^2}+\frac{1}{r}\frac{\partial^2 T}{\partial r}\right]+\mu\left[\frac{\partial u_z}{\partial r}\right]^2 \quad (6)$$

A set of dimensionless variables may now be introduced as follows:

$$Z=\frac{\mu_z}{r_i^2\mu_0\rho} \qquad V=\frac{\rho u_r r_i}{\mu} \qquad R=\frac{r}{r_i} \qquad P=\frac{p}{\rho u_0^{\,2}} \qquad \Pr=\frac{\mu C_P}{\kappa} \qquad U=\frac{u_z}{u_0}$$

$$\theta=\frac{(T-T_{in})}{(T_W-T_{in})} \qquad Ek=\frac{\mu_0^2}{C_P(T_w-T_{in})} \quad (7)$$

The determining equations are then:

$$\frac{1}{R}\frac{\partial(VR)}{\partial R}+\frac{\partial U}{\partial Z}=0 \quad (8)$$

$$V\frac{\partial U}{\partial R}+U\frac{\partial U}{\partial Z}=\frac{-\partial P}{\partial Z}+\frac{\partial^2 U}{\partial R^2}+\frac{1}{R}\frac{\partial U}{\partial R} \quad (9)$$

$$V\frac{\partial \theta}{\partial R}+U\frac{\partial \theta}{\partial Z}=\frac{1}{\Pr}\left[\frac{\partial^2\theta}{\partial R^2}+\frac{1}{R}\frac{\partial\theta}{\partial R}\right]+Ek\left[\frac{\partial U}{\partial R}\right]^2 \quad (10)$$

4. FINITE DIFFERENCE SOLUTION

It should be noted at this point that it is assumed the input values of velocity and temperature are constant every where to the left of the channel. Following the method of Shohet [8], a mesh network is introduced across the range of the problem figure 2. Note that this mesh covers the entire cross section of the channel path, since there is no center line symmetry in this problem.

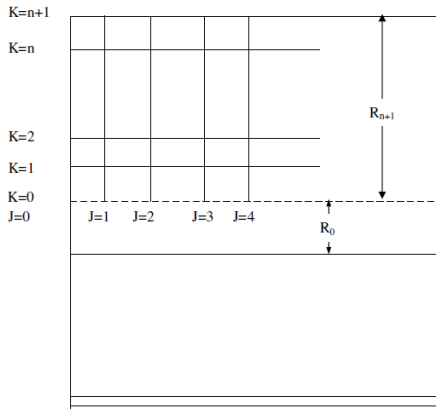

Figure 2: Mesh Scheme

The finite difference approximations to the derivatives in (8) – (10) are shown as follows:

Continuity equation

$$\frac{\partial V}{\partial R}=\frac{V(j+1,k+1)-V(j+1,k)}{\Delta R}$$

$$\frac{\partial U}{\partial Z}=\frac{U(j+1,k+1)+U(j+1,k)-U(j,k+1)-U(j,k)}{2\Delta Z}$$

Momentum equation:

$$\frac{\partial U}{\partial Z}=\frac{U(j+1,k)-U(j,k)}{\Delta Z}$$

$$\frac{\partial U}{\partial R}=\frac{U(j+1,k+1)-U(j+1,k-1)}{2\Delta R}$$

$$\frac{\partial^2 U}{\partial R^2}=\frac{U(j+1,k+1)-2U(j+1,k)+U(j+1,k-1)}{(\Delta R)^2}$$

$$\frac{\partial P}{\partial Z}=\frac{P(j+1)-P(j)}{\Delta Z}$$

Energy equation

$$\frac{\partial \theta}{\partial Z}=\frac{\theta(j+1,\ k)-\theta(j,\ k)}{\Delta Z}$$

$$\frac{\partial \theta}{\partial R}=\frac{\theta(j+1,\ k+1)-\theta(j+1,\ k-1)}{2\Delta R}$$

$$\frac{\partial^2\theta}{\partial R^2} = \frac{\theta(j+1,\, k+1) - 2\theta(j+1,\, k) + \theta(j+1,\, k-1)}{(\Delta R)^2}$$

The finite difference approximations are not perfectly symmetrical nor are they of the same form in all equations. This is done so as to ensure stability of the computer solutions and to enable the equations to be uncoupled from each other. All of these forms approach the real derivative if a small mesh spacing is used.

From the nature of the last three equations it can be seen that (10) is the only expression involving the temperature and therefore, it may be solved separately from (8) and (9). By determining an additional equation involving only unknowns which appear in (9), this equation may be uncoupled from (8) and solved separately. This addition equation or equation of constraint, may be obtained by solving (8) to obtain the velocity at the outer wall *V(j+1, N+1)*, which is zero, in terms of the inner wall velocity *V(j+1, 0)* which is also zero. The resultant equation becomes

$$\sum_{k=1}^{N} R_k U(j+1,k) = \sum_{k=1}^{N} R_k U(j,k) \qquad (11)$$

A set of simultaneous equations (11) together with (9) may be written. One equation can be formed about each mesh point in a column as shown:

$$R_1U(j+1,1) + R_2U(j+1,2) + R_3U(j+1,3) + \text{---------} = \sum_{k=1}^{N} R_k U(j,k),$$

$$\beta_1U(j+1,1) + \gamma_1U(j+1,2) + \text{----------------} + \xi P(j+1) = \phi_1,$$

$$\alpha_2U(j+1,1) + \beta_2U(j+1,2) + \gamma_2U(j+1,3) + \text{---------} + \xi P(j+1) = \phi_2,$$

--- --- --- --- --- --- --- --- --- ---

--- --- --- --- --- --- --- --- --- ---

$$\alpha_NU(j+1,N-1) + \beta_NU(j+1,N) + \text{----------} + \xi P(j+1) = \phi_N,$$

where

$$\alpha_k = \left[\frac{1}{(\Delta R)^2} + \frac{V(j,k)}{2\Delta R} - \frac{1}{2\Delta R R_k}\right], \qquad \beta_k = -\left[\frac{2}{(\Delta R)^2} + \frac{U(j,k)}{\Delta Z}\right]$$

$$\gamma_k = \left[\frac{1}{(\Delta R)^2} + \frac{V(j,k)}{2\Delta R} + \frac{1}{2\Delta R R_k}\right], \qquad \xi = \frac{-1}{\Delta Z} \quad \phi_k = -\left[\frac{P(j)+U^2(j,k)}{\Delta Z}\right]$$

This set of equations can be solved by Gauss-Jordan method. Application of the newly found axial velocities (U's) together with those in the column behind into determines the new transverse velocities (V's).

The set of velocities are now placed into a set of finite difference equations written about each mesh point in a column for equation (10) as shown:

$$\bar{\beta}_1\theta(j+1,1) + \bar{\gamma}_1\theta(j+1,2) + \text{----------} = \bar{\phi}_1 - \bar{\alpha}_1,$$

$$\bar{\alpha}_2\theta(j+1,1) + \bar{\beta}_2\theta(j+1,2) + \bar{\gamma}_2\theta(j+1,3) + \text{----------} = \bar{\phi}_2,$$

--- --- --- --- --- --- --- --- --- ---

--- --- --- --- --- --- --- --- --- ---

$$\bar{\alpha}_N\theta(j+1,N-1) + \bar{\beta}_N\theta(j+1,N) = \bar{\phi}_N - \bar{\gamma}_N,$$

Where

$$\bar{\alpha}_k = \frac{1}{\Pr(\Delta R)^2} + \frac{V(j,k)}{2\Delta R} - \frac{1}{2R_k\Delta R\Pr}, \qquad \bar{\beta}_k = -\left[\frac{2}{\Pr(\Delta R)^2} + \frac{U(j,k)}{\Delta Z}\right],$$

$$\bar{\gamma}_k = \frac{1}{\Pr(\Delta R)^2} - \frac{V(j,k)}{2\Delta R} + \frac{1}{2R_k\Delta R\Pr}$$

$$\bar{\phi}_k = -\left[\frac{U(j,k)\ \theta(j,k)}{\Delta Z} + Ek\left(\frac{U(j+1,k+1) - U(j+1,k-1)}{2\Delta R}\right)^2\right]$$

The same techniques may be used to solve this set of equations as were used to solve the momentum equation.

A difficulty with the continuity equation makes itself evident at this point. Any small round off error in the U velocities near the walls of the channel results in this error being propagated upwards to each V velocity as the continuity equation is marched up the column. This effect is especially noticeable at those mesh points very near the entrance, where the U velocities are

nearly uniform. The result of difficulty is V velocities which adversely affect the succeeding computations.

This effect is generally small in the plane channel case for two reasons. The first is that because only half of the channel is considered, there are fewer equations in which to have the error build up. The second reason is that the center line V velocity is always identically equal to zero and therefore there is no initial error in the continuity equation for each column.

To correct this effect a second finite difference continuity equation is written which is biased "downward". The V velocities are then computed twice by using the original "Upward" equation (12) and the downward equation (13) separately. The V velocities are then averaged at each point and the results are used for the next calculation.

The upward equation is

$$V(j+1,k+1)=$$

$$\frac{1}{R_{k+1}}\left[R_k V(j+1,k)-\frac{\Delta R}{2\Delta Z}\left(U(j+1,k+1)-U(j,k+1)\right)R_{k+1}+R_k\left(U(j+1,k)-U(j,k)\right)\right] \quad (12)$$

and the downward equation is

$$V(j+1,k-1)=$$

$$\frac{1}{R_{k-1}}\left[R_k V(j+1,k)+\frac{\Delta R}{2\Delta Z}\left(R_k U(j+1,k)-U(j,k)\right)+R_{k-1}\left(U(j+1,k-1)-U(j,k-1)\right)\right] \quad (13)$$

5 RESULTS AND DISCUSSION

This paper deals with the motion of a laminar conducting flow in the entrance region of an annual channel with dissipation. Both the velocity and temperature profiles are initially flat while entering the channel. The following initial values are taken at entrance: Z=0; U=1; T=0.1357; V=0 and Pr = 0.1 and different Ek number. Calculations have been carried out till a developed flow is obtained. For fully developed flow calculations have been carried. Figures 3 to 11 show the velocity profile, Figures 12 to 17 show the temperature profile and Figures 18 and 19 show the pressure profile are obtained for different Eckert Number Ek in the annular channel.

Figures 3 to 4, it is observed that as Z increases the velocity decreases for R=1.1; 1.3 and then starts increasing, there after R=1.5 the values of the velocity are less than those of R = 1.5. In this process the velocity starts decreasing for R=1.9 as Z is increases. The velocity profiles are not effects for increasing Eckert number Ek and for fixed Prandtl number.

We also notice that the temperature profiles show that, it reduces initially and then gradually with increasing R. The temperature increases with Z for all cross sections R = constant. The temperature profile follows a parabolic path minimum attained near R=1.5 for Z=0.001. As Z increases the parabolic profile platens and finally becomes a linear path for Z=0.1. These similar observations were obtained for the different values of R and fixing the other parameters. The temperature profiles are effect for increasing Eckert number Ek and for fixed Prandtl Number Pr.

Figure 22 shows pressure profiles for fixed Prandtl Number Pr. The pressure profiles are not effect for increasing Eckert number Ek and for fixed Prandtl Number Pr.

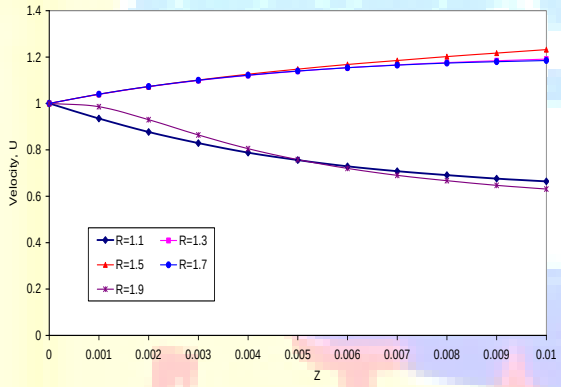

Figure 3: Velocity profile for fixed R

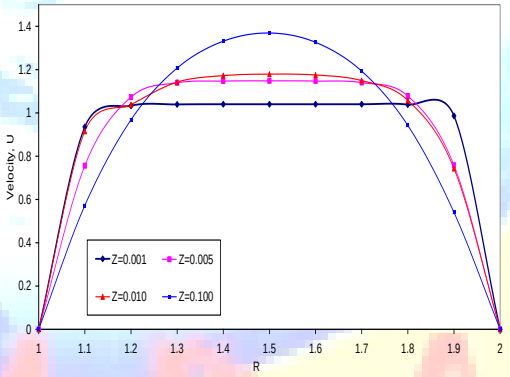

Figure 4: Velocity profile for fixed Z

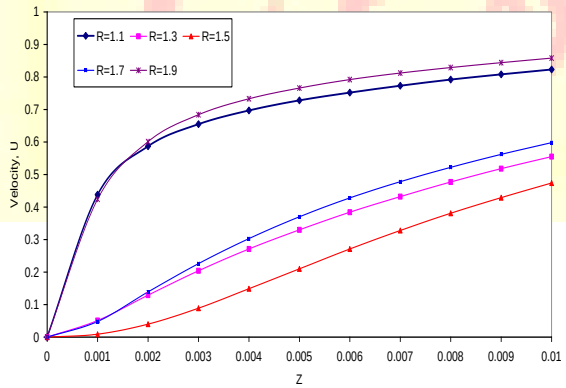

Figure 5: Temperature profile for fixed Ek=0

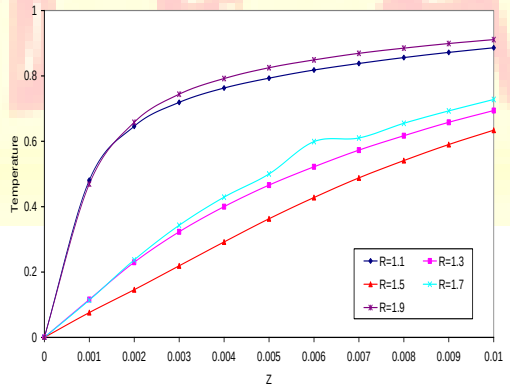

Figure 6: Temperature profile for fixed Ek=1

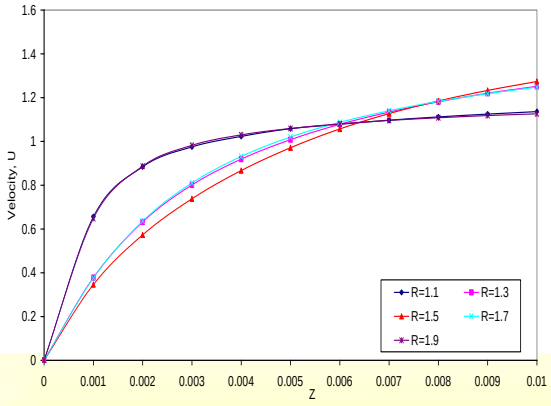

Figure 7: Temperature profile for fixed Ek=5

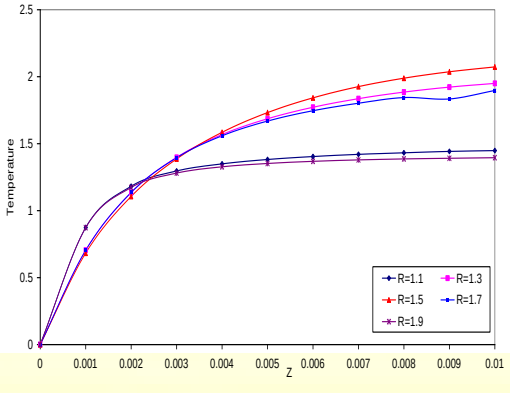

Figure 8: Temperature profile for fixed Ek=10

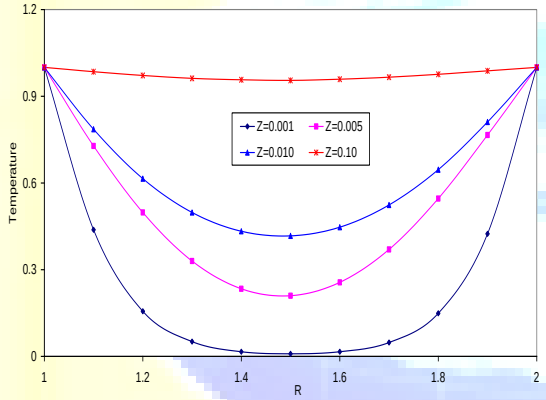

Figure 9: Temperature profile for fixed Ek=0

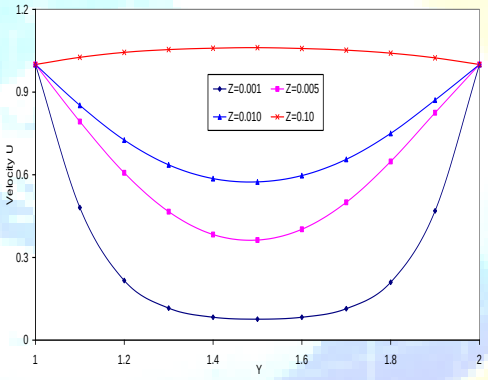

Figure 10: Temperature profile for fixed Ek=1

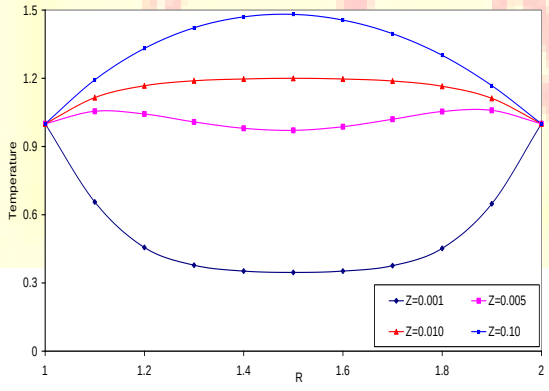

Figure 11: Temperature profile for fixed Ek=5

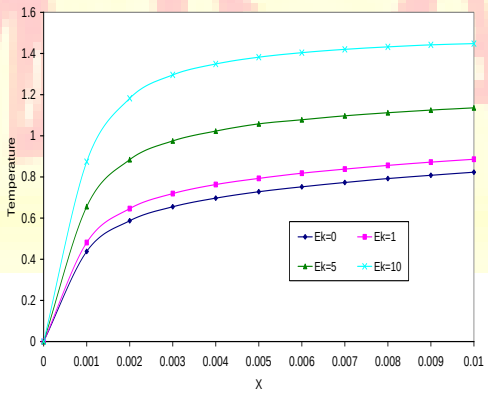

Figure 12: Temperature profile for fixed Ek=10

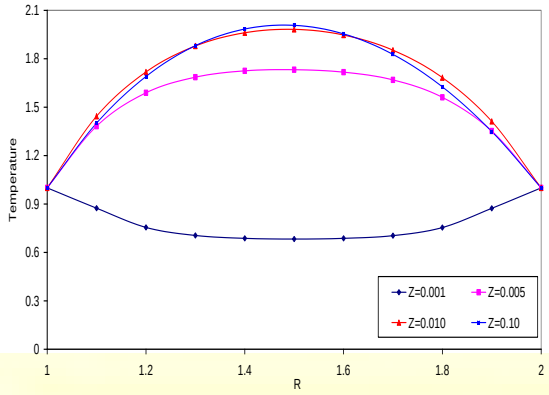

Figure 13: Temperature profile for fixed R=1.1

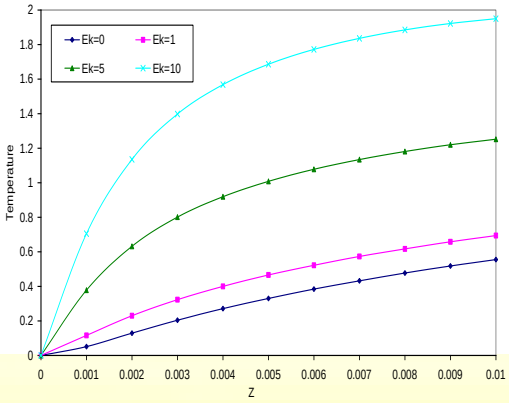

Figure 14: Temperature profile for fixed R=1.3

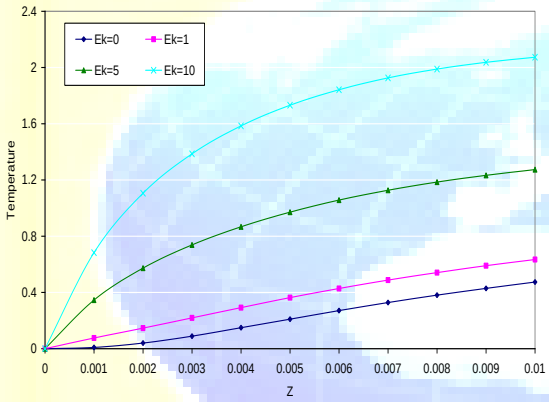

Figure 15: Temperature profile for fixed R=1.5

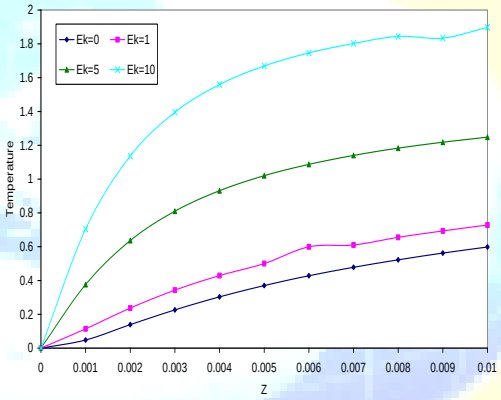

Figure 16: Temperature profile for fixed R=1.7

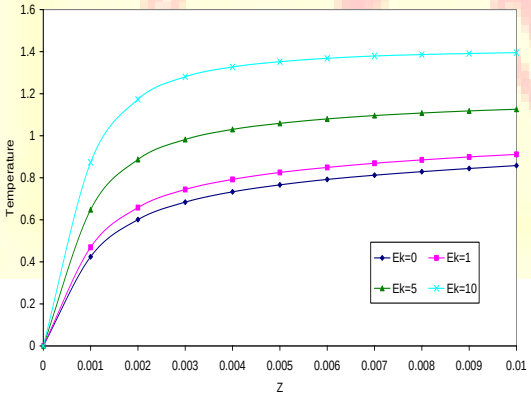

Figure 17: Temperature profile for fixed R=1.9

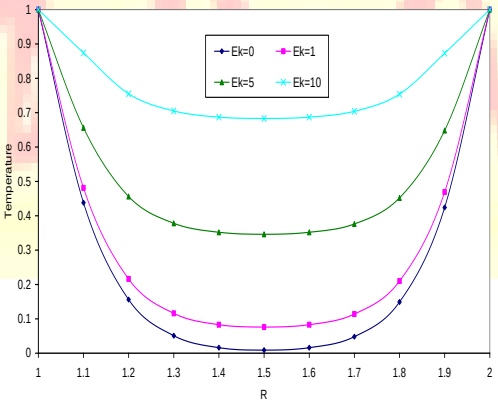

Figure 18: Temperature profile for fixed Z=0.001

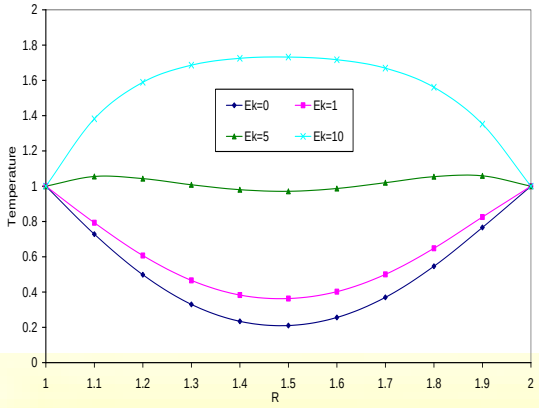

Figure 19: Temperature profile for fixed Z=0.005

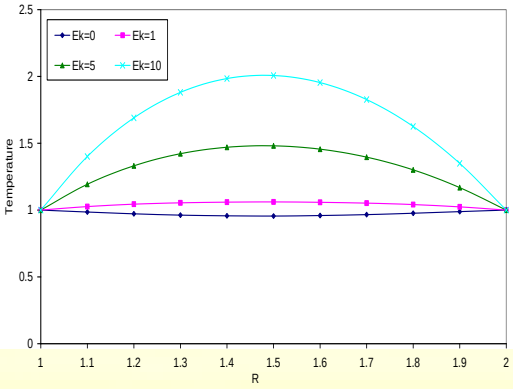

Figure 20: Temperature profile for fixed Z=0.01

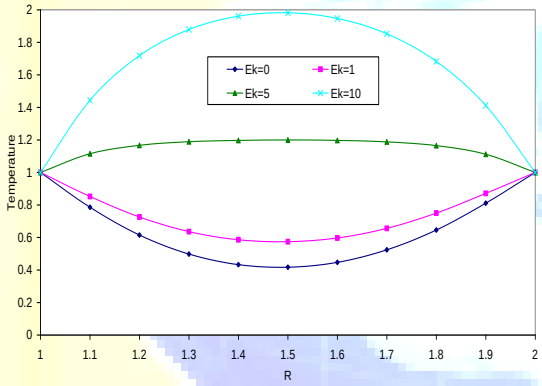

Figure 21: Temperature profile for fixed Z=0.01

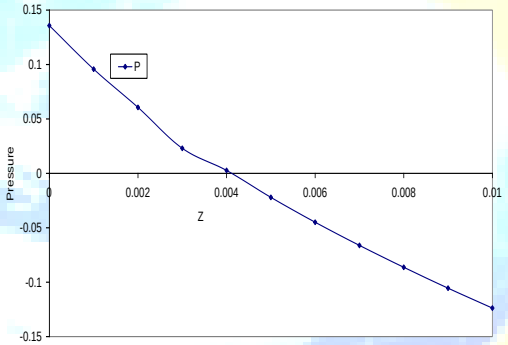

Figure 22: Pressure profile

REFERENCE

1. Beavers, G. S., Sparrow, E. M., and Magnuson, R. B., Int. J. Heat Mass Transfer, vol. 13, no. 4, pp. 689–675, 1970.
2. Ben-Ali,T. M., Soliman, H. M., and Zaiffeh, E. K., ASME J. Heat Transfer, vol. 111, no. 4, pp. 1090–1093, 1989.
3. Carnavos,T. C., Heat Transfer Eng., vol. 1, no. 2, pp. 41–46, 1979.
4. Chiranjivi, C., and Vidyanidhi, V., Indian Chem. Eng., vol. 15, no. 1, pp. 49–51, 1973.
5. Chung, B. T. F., and Hsia, R. P., Heat Transfer Eng., vol. 15, no. 4, pp. 55–65, 1994.
6. Helmut, F. B., Int. J. Heat Mass Transfer, vol. 31, no. 7, pp. 1451–1469, 1988.
7. Hsieh, S. S., and Wen, M. Y., Int. J. Heat Mass Transfer, vol. 39, no. 2, pp. 299–310, 1996.

8. Incropera,F. P., and DeWitt, D. P., Introduction to Heat Transfer, 3rd ed.,Wiley, p. 411, New York, 1996.
9. Kelkar, K. M., and Patankar, S. V., ASME J. Heat Transfer, vol. 112, no. 2, pp. 342–348, 1990.
10. Lei, Q. M., and Trupp, A. C., ASME J. Heat Transfer, vol. 111, no. 4, pp. 1088–1090, 1989.
11. Lin, C. X., Zhang, P., and Ebadian, M. A., Int. J. Heat Mass Transfer, vol. 40, no. 14, pp. 3293–3304, 1997.
12. Muzychka, Y.S. and Yovanovich M.M., ASME J. Heat Transf., 126, p.54, 2004.
13. Muzychka, Y.S. and Yovanovich M.M., in Compact Heat Exchangers, edited by Cleata G.P., Thonon B., Bontemps, A., and Kandlikar, S. (A Festchrift on the 60th Birth Day of Ramesh K. Shah, Grenoble, Frnace), p.123, 2002.
14. Muzychka, Y.S. and Yovanovich M.M., in Compact Heat Exchangers, edited by Cleata G.P., Thonon B., Bontemps, A., and Kandlikar, S. (A Festchrift on the 60th Birth Day of Ramesh K. Shah, Grenoble, Frnace), p.131, 2002.
15. Nida, T., Int. Chem. Eng., vol. 20, no. 2, pp. 258–265, 1980.
16. Patankar, S. V., and Spalding, D. B., Int. J. Heat Mass Transfer, vol. 15, no. 10, pp. 1787–1806, 1972.
17. Patankar, S. V., Ivanovic, M., and Sparrow, E. M., ASME J. Heat Transfer, vol. 101, no. 1, pp. 29–37, 1979.
18. Prakash, C., and Liu, Ye-Di, ASME J. Heat Transfer, vol. 107, no. 1, pp. 84–91, 1985.
19. Rustman, I. M., and Soliman, H. M., ASMEJ. Heat Transfer, vol. 110, no. 2, pp. 310–313, 1988.
20. Shah, R. K., and London, A. L., Laminar Flow Forced Convection in Ducts, Academic Press, New York, 1978.
21. Soliman, H. M., and Feinglod, A., Proc. 6th Int. Heat Transfer Conf., Toronto, Canada, vol. 2, pp. 571–576, 1978.
22. Soliman, H. M., and Feingold,A., Chem. Eng. J., vol. 14, no. 2, pp. 119 - 128, 1977.
23. Soliman, H. M., ASME J. Heat Transfer, vol. 109, no. 1, pp. 247–249, 1987.
24. Soliman, H. M., Chau,T. S., and Trupp,A. C., ASME J. Heat Transfer, vol. 102, no. 4, pp. 598–604, 1980.

25. Sparrow, E. M., Chen, T. S., and Tonsson,V. K., Int. J. Heat Mass Transfer, vol. 7, no. 5, pp. 583–585, 1964.
26. Tao, W. Q., ASME J. Heat Transfer, vol. 109, no. 3, pp. 791–795, 1987.
27. Trupp, A. C., and Lau, A. C., ASME J. Heat Transfer, vol. 106, no. 2, pp. 467–469, 1984.
28. Üzun, I and Unsal, M., Int. Comm.H.M.T, 24, p.835, 1997.
29. Uzun, I., and Unsal, M., Int. Commun. Heat Mass Transfer, vol. 24, no. 6, pp. 835–848, 1997.
30. Uzun, I., Turkish J. Eng. Env. Sci., 26, p.7, 2002.